PCP
PLANT & CELL PHYSIOLOGY

Regular Paper

ABCG15 Encodes an ABC Transporter Protein, and is Essential for Post-Meiotic Anther and Pollen Exine Development in Rice

Peng Qin[1,2,4], Bin Tu[1,4,5], Yuping Wang[1,2,4], Luchang Deng[1,2], Teagen D. Quilichini[3], Ting Li[1,2], Hui Wang[1], Bingtian Ma[1] and Shigui Li[1,2,*]

[1]Rice Research Institute of Sichuan Agricultural University, Chengdu Wenjiang, Sichuan, 611130, PR China
[2]State Key Laboratory of Hybrid Rice, Sichuan Agricultural University, Chengdu Wenjiang, Sichuan, 611130, PR China
[3]Department of Botany, University of British Columbia, Vancouver, British Columbia V6T 1Z4, Canada
[4]These authors contributed equally to this work.
[5]Present address: Department of Botany and Plant Sciences, Institute of Integrative Genome Biology, University of California, Riverside, CA 92521, USA.
*Corresponding author: E-mail, lishigui@sicau.edu.cn; Fax, +86-28-86290897.
(Received September 11, 2012; Accepted November 25, 2012)

In flowering plants, anther and pollen development is critical for male reproductive success. The anther cuticle and pollen exine play an essential role, and in many cereals, such as rice, orbicules/ubisch bodies are also thought to be important for pollen development. The formation of the anther cuticle, exine and orbicules is associated with the biosynthesis and transport of wax, cutin and sporopollenin components. Recently, progress has been made in understanding the biosynthesis of sporopollenin and cutin components in Arabidopsis and rice, but less is known about the mechanisms by which they are transported to the sites of deposition. Here, we report that the rice ATP-binding cassette (ABC) transporter, *ABCG15*, is essential for post-meiotic anther and pollen development, and is proposed to play a role in the transport of rice anther cuticle and sporopollenin precursors. *ABCG15* is highly expressed in the tapetum at the young microspore stage, and the *abcg15* mutant exhibits small, white anthers lacking mature pollen, lipidic cuticle, orbicules and pollen exine. Gas chromatography—mass spectrometry (GC-MS) analysis of the *abcg15* anther cuticle revealed significant reductions in a number of wax components and aliphatic cutin monomers. The expression level of genes involved in lipid metabolism in the *abcg15* mutant was significantly different from their levels in the wild type, possibly due to perturbations in the homeostasis of anther lipid metabolism. Our study provides new insights for understanding the molecular mechanism of the formation of the anther cuticle, orbicules and pollen wall, as well as the machinery for lipid metabolism in rice anthers.

Keywords: ABC transporter • Anther • Male sterility • Pollen exine • Rice.

Abbreviations: ABC, ATP-binding cassette; GC-MS, gas chromatography–mass spectrometry; LTP, lipid transfer protein; MMC, microspore mother cell; qPCR, quantitative PCR; RT–PCR, reverse transcription–PCR; SEM, scanning electron microsocpy; TEM, transmission electron microscopy.

Introduction

Anther development, including the differentiation of specialized tissues necessary for the formation of pollen grains, is an important and complex biological process in flowering plants (McCormick 1993, Scott et al. 2004). A typical anther contains four layers of cells: the epidermis, the endothecium, the middle layer and the tapetum. In the center of each anther lobe, microsporocytes develop into mature pollen grains by undergoing meiosis followed by two mitotic divisions.

The anther cuticle consists of cutin and wax, and plays an important role in anther and pollen development (Li and Zhang 2010). Cutin is a polyester consisting mainly of ω- and mid-chain hydroxy and epoxy C16–C18 fatty acids. Cuticular wax is a mixture of unbranched aliphatic compounds having 20–60 carbons and may include some secondary metabolites, e.g. triterpenoids and flavonoids (Samuels et al. 2008). Recently, several genes have been identified that are important for anther cuticle formation in rice, including *WDA1* (*Wax-Deficient Anther1*) (Jung et al. 2006), *CYP704B2* (Li et al. 2010), *TDR* (*Tapetum Degeneration Retardation*) (Li et al. 2006), *DPW* (*Defective Pollen Wall*) (Shi et al. 2011) and *UDT1* (*Undeveloped Tapetum1*) (Jung et al. 2005). However, the molecular mechanism of anther cuticle formation in rice remains unknown.

Pollen exine plays a critical role in pollen grain formation. The main constituent of the exine is the tough biopolymer sporopollenin, which is thought to be made up of aliphatic and aromatic constituents (Hemsley 1994, Ahlers et al. 1999, Ahlers et al. 2000, Ahlers et al. 2003, Dobritsa et al. 2010,

Plant Cell Physiol. 54(1): 138–154 (2013) doi:10.1093/pcp/pcs162, available online at www.pcp.oxfordjournals.org

Ariizumi and Toriyama 2011). Recent genetic and biochemical studies have shown that a number of genes are essential for exine formation, e.g. *WDA1* (Jung et al. 2006), *CYP704B2* (Li et al. 2010), *TDR* (Li et al. 2006), *GAMYB* (Aya et al. 2009, Liu et al. 2010) and *DPW* (Shi et al. 2011) in rice, and *NEF1* (*No Exine Formation1*) (Ariizumi et al. 2004), *MS2* (Aarts et al. 1997, Dobritsa et al. 2009, G. Chen et al. 2011), *CYP704B1* (Dobritsa et al. 2009), *CYP703A2* (Dobritsa et al. 2009), *ACOS5* (*Acyl-CoA synthetase* 5) (de Azevedo Souza et al. 2009), *LAP5/PSKB*, *LAP6/PSKA* (Dobritsa et al. 2010, Kim et al. 2010), *TKPR1/2* (*Tetraketide α-pyrone Reductase1/2*) (Grienenberger et al. 2010) and *ABCG26* (*ATP-binding cassette transporter G26*) (Quilichini et al. 2010) in Arabidopsis. Many of these proteins were proposed to be involved in lipid metabolism, and play an important role during pollen exine formation. *OsC6*, encoding a lipid transfer protein in rice (Zhang et al. 2010), and *ABCG26/WBC27*, encoding an ATP-binding cassette transport protein in Arabidopsis (Quilichini et al. 2010, Choi et al. 2011, Dou et al. 2011), were proposed to be critical for the export and translocation of sporopollenin precursors from their site of synthesis in the tapetum. However, the molecular mechanisms underlying anther cuticle, orbicule and exine formation are still largely unknown.

ATP-binding cassette (ABC) transporter proteins belong to a large, diverse and ubiquitous superfamily (Rea 2007). The main function of ABC transporter proteins is to participate directly in the active transport of a wide range of molecules across membranes (Markus 2006). In plants, the ABC transporter genes are particularly abundant. The Arabidopsis and rice genomes encode 130 and 132 members, respectively, and their encoded proteins are categorized into different subfamilies (Verrier 2008, Verrier et al. 2008). The ABCG subfamily, the largest subfamily both in rice and in Arabidopsis, contains the former white/brown complex (WBC) and pleiotropic drug resistance (PDR) groups, which encode half-size and full-size ABC transporter proteins, respectively. The half-size ABCG transporters must form homodimers or heterodimers with other half-molecule transporters to be functional ABC transporters (Rea 2007). Recent studies showed that members of the G subfamily are critical for fatty acid export, ABA response and pathogen resistance. *ABCG11/WBC11/DSO*, *ABCG12/CER5*, *ABCG13*, *ABCG32/PEC1* and *OsABCG31/HvABCG31* (Pighin et al. 2004, Bird et al. 2007, Panikashvili et al. 2007, Panikashvili et al. 2010, Bessire et al. 2011, W. Chen et al. 2011, Panikashvili et al. 2011) were reported to be required for lipid export. *ABCG26/WBC27* is proposed to be essential for the export of sporopollenin precursors (Quilichini et al. 2010, Choi et al. 2011), whereas *ABCG25*, *ABCG40/PDR12* and *AtABCG22* are involved in ABA responses (Kang et al. 2010, Kuromori et al. 2010, Kuromori et al. 2011). However, the function of many ABCG transporters remains unknown.

In this study, we identified a male-sterile line of rice caused by a spontaneous mutation in an ABC transporter gene, *ABCG15*, and report its key roles in post-meiotic anther and pollen development. *ABCG15* is highly expressed in the tapetum at the young microspore stage. It is essential for the formation of anther cuticle, orbicules and pollen exine by putatively affecting the transport of wax, cutin and sporopollenin precursors. In the mutant *abcg15*, monomers of cutin and wax are significantly decreased, and a glossy anther epidermal surface, as well as an absence of orbicules and exine leads to a male-sterile phenotype. This work provides new insights into mechanisms of anther and pollen development, and broadens our knowledge of the regulation of lipid metabolite export.

Results

Anther cuticle, orbicule and exine formation is impaired in *abcg15*

The h_2s mutant is a spontaneous mutant obtained from *indica* rice *Chuannong H2S*. The mutant h_2s displays shorter, white anthers without mature pollen, but no obvious defect in vegetative growth (**Fig. 1A–E**). H_2S was renamed *ABCG15* after a 12 nucleotide deletion was found in a putative ABC transporter gene (*ABCG15*) in the h_2s mutant, according to map-based cloning (see below).

To characterize the anther morphological defects in *abcg15*, we performed semi-thin section analysis for the anthers of the wild type and *abcg15*. Based on the previous classification of rice pollen development (Feng et al. 2001, Jung et al. 2006), we delineated anther development into six stages, namely early meiosis stage, meiosis stage, post-meiosis stage, young microspore stage, vacuolated pollen stage and late mitosis stage (**Fig. 2A–C, G–I**). No defect was observed at the early meiosis stage in *abcg15* (**Fig. 2A, D**). Subsequently, microspore mother cells (MMCs) underwent meiosis in the wild type and *abcg15*, to form the tetrads at meiosis stage with all four layers of cells appearing normal (**Fig. 2B, E**). 4′,6-Diamidino-2-phenylindole staining also indicated that chromosomes separated normally during meiosis in *abcg15* (data not shown).

Up to the end of meiosis, tetrads had begun to deposit primexine and showed a clear boundary around microspores. In the meantime, tapetal cells started to degrade and became condensed and deeply stained (**Fig. 2C**). The tetrads in *abcg15* did not show any clear boundary (primexine) surrounding pollen microspores, as seen in the wild type (**Fig. 2F**). The *abcg15* tapetum did not become condensed, but rather appeared swollen and vacuolated (**Fig. 2F**). At the young microspore stage in the wild type, pollen grains with visible exine were released into the anther locule and the tapetum continued to become condensed (**Fig. 2G**). In contrast, *abcg15* showed no obvious pollen exine, and pollen grain degradation was observed in the anther locule (**Fig. 2J**). Delayed degradation of the tapetum was observed in *abcg15*, and the tapetal cells appeared to be lightly stained, vacuolated and swollen (**Fig. 2J**). At the vacuolated pollen and late mitosis stages, wild-type microspores underwent mitosis twice to form mature pollen grains; the tapetum and middle layer degraded (**Fig. 2H, I**). Unlike the wild type, microspores in *abcg15* were completely

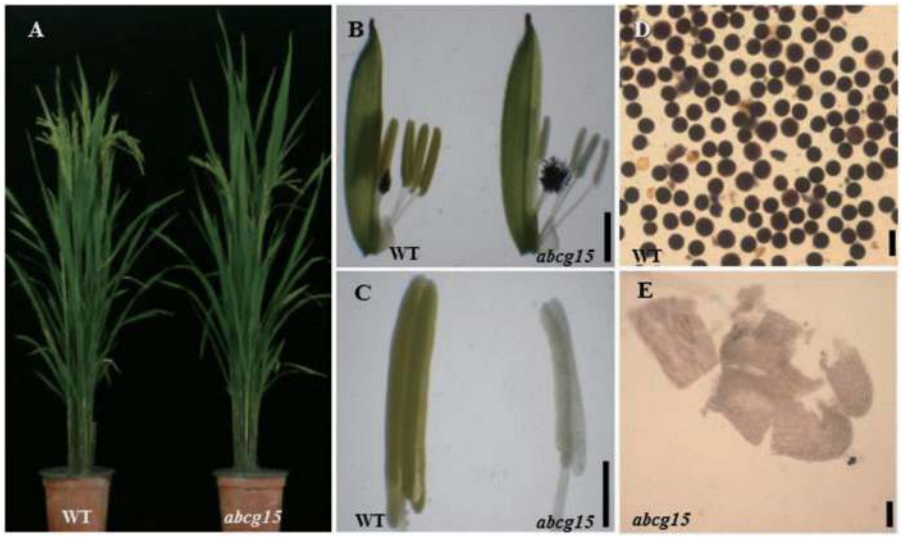

Fig. 1 Phenotypic comparison of the wild type and *abcg15*. (A) Comparison of a wild-type plant (left) and an *abcg15* plant (right). (B) Comparison of a wild-type floret (left) and an *abcg15* floret (right) at the heading stage. (C) Comparison of a wild-type anther (left) and an *abcg15* anther (right) at the mature pollen stage. (D) and (E) I_2–KI pollen staining for the wild type (D) and *abcg15* (E). Bars = 2 mm (B); 0.5 mm (C); 30 μm (D) and (E).

degraded, leaving empty anther locules, although the anthers still maintained a layer of tapetal cells (**Fig. 2K, L**).

To obtain detailed information about anther and pollen development in *abcg15*, we performed transmission electron microscopy (TEM) analysis at four anther development stages (early meiosis stage, post-meiosis stage, young microspore stage and late mitosis stage). At the early meiosis stage, consistent with the semi-thin sections, no significant difference between the wild type and *abcg15* was observed for the epidermis, endothecium, middle layer and tapetal cells (**Fig. 3A, E, I, M, Q, U**). At the post-meiosis stage, the wild-type tapetum became highly condensed (**Fig. 3B**) while the primexine started to form on the surface of tetrads (**Fig. 3J**). In contrast, the tapetum of *abcg15* appeared enlarged (**Fig. 3F**). No normal exine structure was observed on the *abcg15* microspores; only plasma membrane-like structures existed in the locules (**Fig. 3N**). Up to the young microspore stage, similar to thin-section observations, the tapetum became thinner, and its degradation was clearly observed in the wild type (**Fig. 3C**). Meanwhile, many U-shaped orbicules appeared on the locular side of the tapetum, and the primary exine structure, which contained nexine and tectum, was formed on the surface of wild-type microspores (**Fig. 3K**). In contrast, the tapetum in *abcg15* did not become thinner as in the wild type but remained swollen (**Fig. 3G**). On the locular side of tapetal cells in *abcg15*, no obvious orbicules were observed and no exine structures were observed on the aborting microspores (**Fig. 3O**). At the late mitosis stage, the tapetum in the wild type was largely degraded, with only a thin cell layer left (**Fig. 3D**). A typical pollen exine structure with nexine, baculum and tectum on the microspore surface was formed in the wild type at this stage, and the U-shaped orbicules were filled with electron-dense material (**Fig. 3L**). However, the *abcg15* tapetum appeared not to have undergone degradation at the late mitosis stage (**Fig. 3H**), and no pollen exine or U-shaped orbicules were observed (**Fig. 3P**).

In addition to the loss of pollen wall and orbicule formation in *abcg15* mutants, defects in anther epidermal cells were also observed. The cell walls of the anther epidermis in the wild type were lightly stained and covered with a smooth cuticle layer from early meiosis to the post-meiosis stage (**Fig. 3Q, R**). At the young microspore and late mitosis stage, the cuticle in anther epidermal cells was folded and formed nanoridges (**Fig. 3S**), which reached maturity by the late mitosis stage (**Fig. 3T**), and resemble the ridges on petal and sepal epidermal cells in Arabidopsis (Li-Beisson et al. 2009, Panikashvili et al. 2009, Panikashvili et al. 2011). However, in *abcg15*, the cell walls of the anther epidermis appeared electron dense and became thinner from the post-meiosis stage to the late mitosis stage (**Fig. 3V, W, X**). At the young microspore and late mitosis stage, the cuticle of the *abcg15* mutants failed to form nanoridges, and displayed a slightly thinner cuticle (**Fig. 3W, X**).

The ultrastructure of the cuticle is strongly altered in the mutant epidermal cells of anthers

To gain more information about the anther cuticle and orbicule defects observed in the *abcg15* mutant, we used scanning electron microscopy (SEM) on anther samples from different stages of the wild type and *abcg15*. In the wild type, the initial cells in the epidermal cells were formed at the early meiosis stage (**Fig. 4A**). At the post-meiosis stage, distinct epidermal cells with network-forming nanoridges were observed (**Fig. 4B**). At the young microspore and late mitosis stages, the cuticle

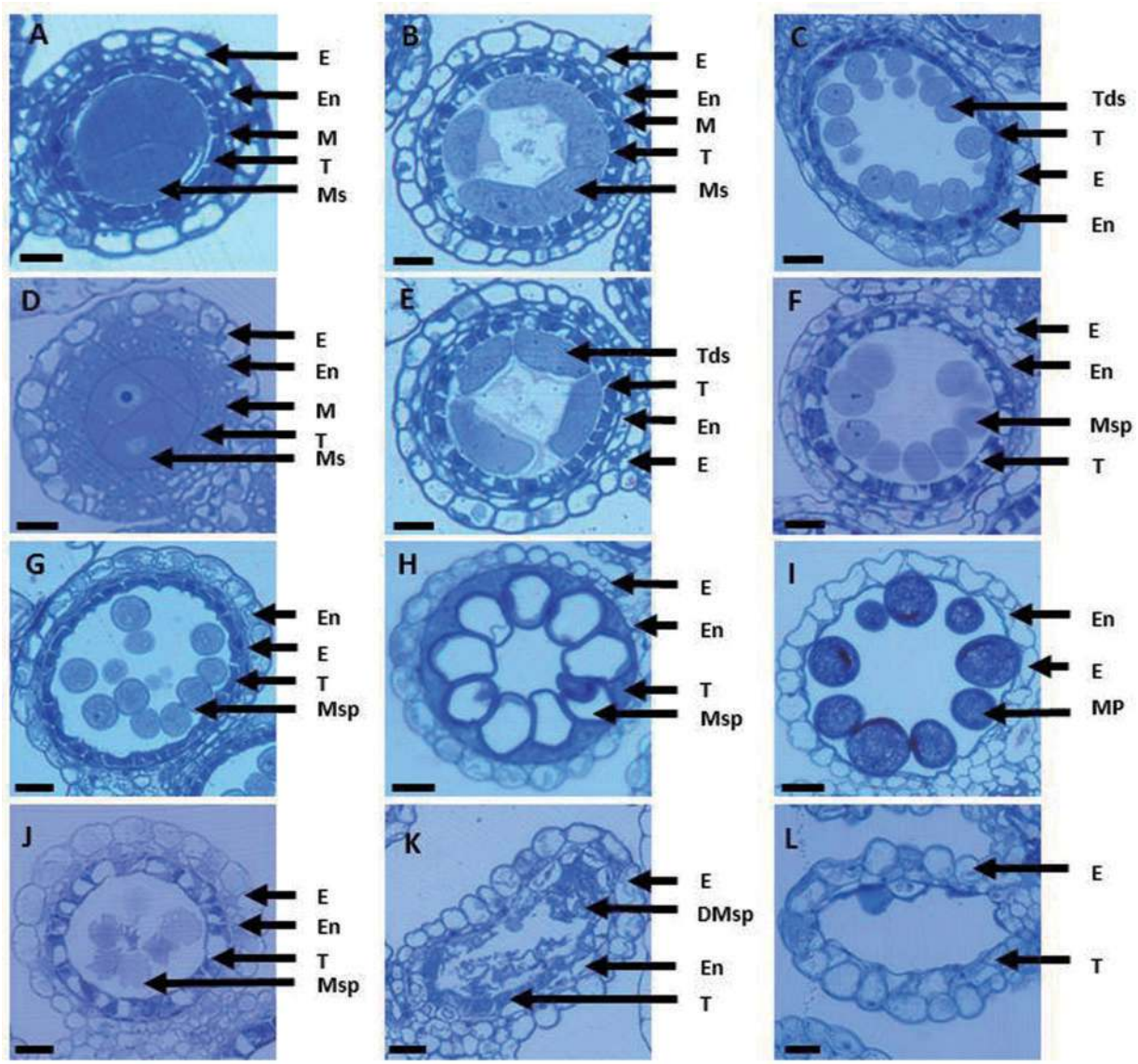

Fig. 2 Semi-thin section comparison of anther development between the wild type and *abcg15*. Six stages of anther development between the wild type and *abcg15* were compared. (A and D) early meiosis stage; (B and E) meiosis stage; (C and F) post-meiosis stage; (G and J) young microspore stage; (H and K) vacuolated pollen stage; (I and L) the late mitosis stage. Wild-type sections are shown in (A–C) and (G–I); the *abcg15* sections are shown in (D–F) and (J–L). DMsp, degenerated microspores; E, epidermis; En, endothecium; M, middle layer; MP, mature pollen; T, tapetum; Ms, microsporocyte; Tds, tetrads; Msp, microspore. Bars = 15 μm.

formed a network of nanoridges on the anther epidermal cell surface in the wild type (**Fig. 4C, D**). Consistent with TEM results, many orbicules were observed in the wild type at the inner locule side of tapetum cells (**Fig. 4E**). Moreover, wild-type epidermal cells gradually appeared wider and longer from the post-meiosis to late mitosis stage. The *abcg15* mutant did not show any obvious differences from the wild type at the early meiosis stage (**Fig. 4F**), but, at the post-meiosis stage, the network-forming nanoridges were not observed on the mutant epidermal cell surface (**Fig. 4G**). Consistent with TEM observations, nanoridges were absent on the epidermal cell surface in *abcg15* at the young microspore stage and the late mitosis stage. Instead, the epidermal cell surfaces were smooth (**Fig. 4H, I**). As observed by TEM, *abcg15* did not form orbicules on the inner side of anther locules (**Fig. 4J**). Moreover, from the post-meiosis stage to the late mitosis stage, the epidermal cells in *abcg15* did not undergo normal development, appearing reduced in length and width, which resulted in shorter and smaller anthers (**Fig. 1C**).

Mapping-based cloning of *ABCG15*

To isolate the gene responsible for the male-sterile phenotype, map-based cloning was employed. Our previous genetic

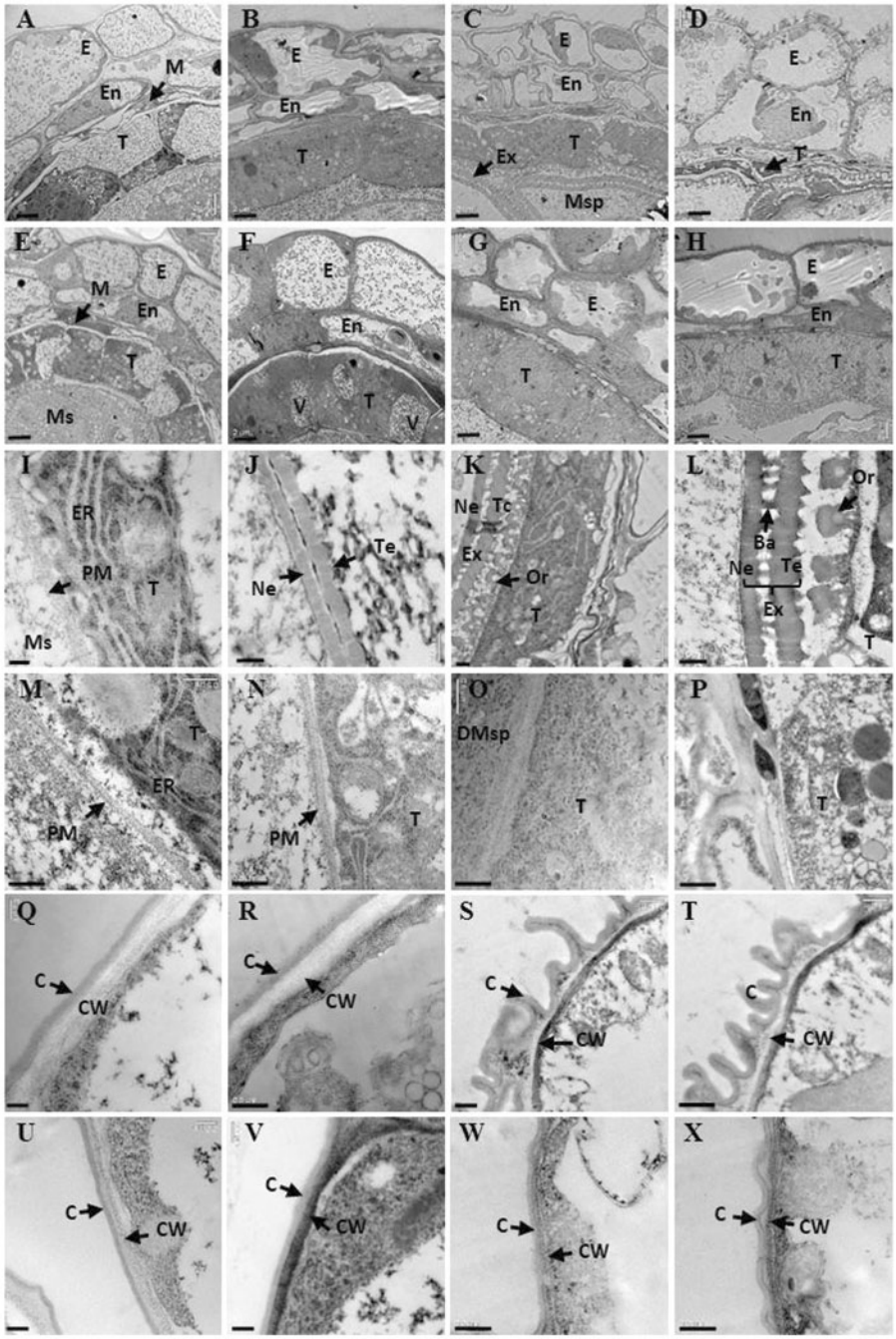

Fig. 3 TEM comparison of anthers between the wild type and *abcg15*. Four layers of anther, pollen exine, orbicules and cuticle at four stages of anther development were compared between the wild type and *abcg15*. (A), (E), (I), (M), (Q) and (U), early meiosis stage; (B), (F), (J), (N), (R) and (V), post-meiosis stage; (C), (G), (K), (Q), (S) and (W), vacuolated pollen stage; (D), (H), (L), (P), (T) and (X), late mitosis stage. (A–D) and (E–H) show four layers of wild-type and *abcg15* anthers, respectively. (I–L) and (M–P) show pollen exine development of the wild type and *abcg15*, respectively. (Q–T) and (U–X) show anther epidermis cuticle formation of the wild type and *abcg15*, respectively. Ba, bacula; C, cuticle; CW, cell wall; DMsp, degenerated microspores; E, epidermis; En, endothecium; ER, endoplasmic reticulum; Ex, exine; M, middle layer; Ne, nexine; Ms, microsporocyte; Msp, microspore; Or, orbicules; T, tapetum; Tds, tetrads; Te, tectum; PM, plasma membrane; V, vacuole. Bars = 0.2 μm in (I), (J), (Q), (S), (U) and (V); 0.5 μm in (L–P), (R), (T),(W) and (X); 1 μm in (K), 2 μm in (A–H).

analysis indicated that the mutant phenotype was controlled by a single recessive nuclear locus. According to primary mapping results, the mutant gene was located between the markers RM454 and RM528 on chromosome 6. In order to map the mutation further, F_2 mapping populations of 3,400 individuals generated from the cross between the mutant and *9311* (*Indica*) or of 2,400 individuals generated from the cross between the mutant and *Nipponbare* (*Japonica*) were analyzed

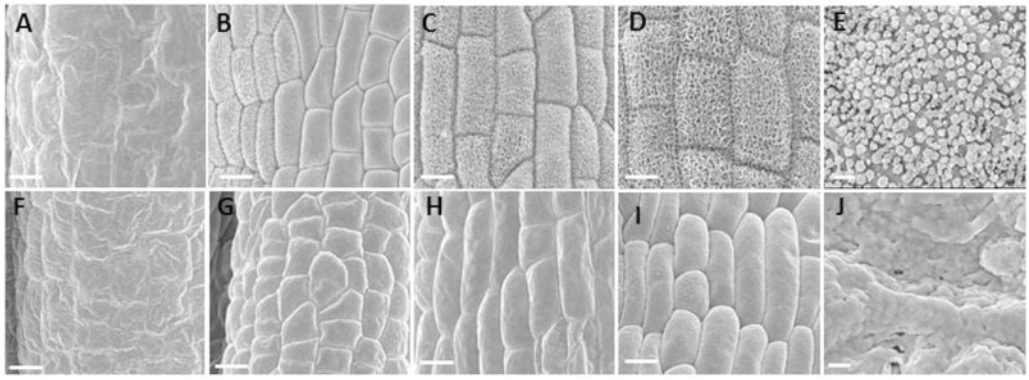

Fig. 4 SEM observation for wild-type and *abcg15* anther surface and orbicules. (A–E) Wild-type anther epidermis and orbicules (E). (F–J) *abcg15* mutant anther epidermis and orbicules (J). At early meiosis (A and F) and post-meiosis (B and G), no obvious difference in the anther cuticle between the wild type and *abcg15* was observed. At the young microspore stage (C and H) and late mitosis stage (D and I), the *abcg15* mutant (H and I) showed a glossy epidermis without cuticle compared with the wild type (C and D). The absence of orbicules was observed in *abcg15* at the mature pollen stage (J). Bars = 10 μm in (A–D) and (F–I), 2.5 μm in (E) and (J).

using a set of primer pairs. The gene was finally mapped to a 50 kb region on chromosome 6 between the marker RM20366 and a newly developed marker Indel40520, with one recombinant for each marker (**Fig. 5A**). Seven genes were annotated within that region in the Rice Genome Annotation Project (http://rice.plantbiology.msu.edu/pseudomolecules) (**Supplementary Table S3**). To determine which gene was responsible for the observed phenotype, we investigated the expression pattern of the seven candidate genes in the rice anther gene expression database (http://rice.sinica.edu.tw/rice/) (C.F. Huang et al. 2009). Only *Loc_Os06g40550* was highly and specifically expressed at the anther tetrad stage. As the mutant showed defective development around the tetrad stage, we selected *Loc_Os06g40550* as the best candidate for further study. Both genomic DNA and cDNA from the mutant displayed a 12 nucleotide deletion at the predicted fifth exon of *Loc_Os06g40550* which does not change the RNA coding frame (**Fig. 5B, C**). The leucine (one of the four amino acid encoded by those 12 nucleotides) was conserved among 16 species (**Supplementary Fig. S1**), indicating that the deleted leucine might be important for *Loc_Os06g40550* function. *Loc_Os06g40550* encodes a protein with an ABC transporter domain, and is a putative ortholog of Arabidopsis *ABCG26/WBC27*. The mutant of *ABCG26/WBC27* exhibits male sterility because of the loss of pollen exine formation (Quilichini et al. 2010, Choi et al. 2011, Dou et al. 2011); therefore, *Loc_Os06g40550* was the best candidate involved in anther cuticle and pollen wall formation. *Loc_Os06g40550* was named *ABCG15* according to the nomenclature of plant ABC transporter proteins (Verrier 2008, Verrier et al. 2008).

To confirm that the mutation in *Loc_Os06g40550/ABCG15* was responsible for the male-sterile phenotype, a binary construct with a 8,219 bp wild-type genomic DNA fragment containing *Loc_Os06g40550* was generated, and transformed into the calli induced from young panicles of the mutant. The recovered male fertility, anther length and pollen fertility in transgenic plants indicated that the 12 bp deletion in *Loc_Os6g40550* was responsible for the phenotype in *abcg15* (**Supplementary Fig. S2**).

ABCG15 is conserved in embryophytes

ABCG15 is predicted to encode an ABC transporter protein (http://rice.plantbiology.msu.edu/), which belongs to the G subfamily of the rice ABC transporter superfamily. The G subfamily has 50 members, which are grouped into half-size and full-size transport proteins (**Supplementary Fig. S3**). ABCG15 belongs to the half-size group. Phylogenetic analysis showed that ABCG15 shares 15–50% amino acid identity with all G subfamily members, and forms a subclade with OsABCG18, OsABCG27 and OsABCG4 (**Supplementary Fig. S3**), which share ∼44% amino acid identity with ABCG15. The functions of OsABCG27, OsABCG18, OsABCG4 are not known, but *AtABCG25* and *AtABCG22*, the Arabidopsis homologs of *OsABCG27* and *OsABCG4*, are involved in the ABA response to temperature stress (Baron et al. 2012) or drought stress (Gonzalez et al. 2012), respectively.

To gain further information about the potential function of ABCG15, we performed bioinformatic analyses with the ABCG15 full-length protein sequence as a query to search for the closest relatives, using a Phytozome blast search with default parameters (http://www.phytozome.net). Twenty-five annotated protein sequences related to ABCG15 were obtained from different species, all of which were predicted to be ABC transporters. The alignment for the blast hit sequences showed that most amino acids are conserved among different species, including the ABC transporter domain (**Supplementary Fig. S1**). These ABCG15-related sequences grouped into three clades (I, II and III) (**Fig. 6**). The species in clade I and II belong to dicotyledons and monocotyledons, respectively, and the species in clade III belong to mosses and pteridophytes. ABCG15 shared ∼60, ∼80 and ∼50% identity with those ABCG15-related protein sequences in monocots, dicots and clade III (*Selaginella moellendorffii* and *Physcomitrella patens*),

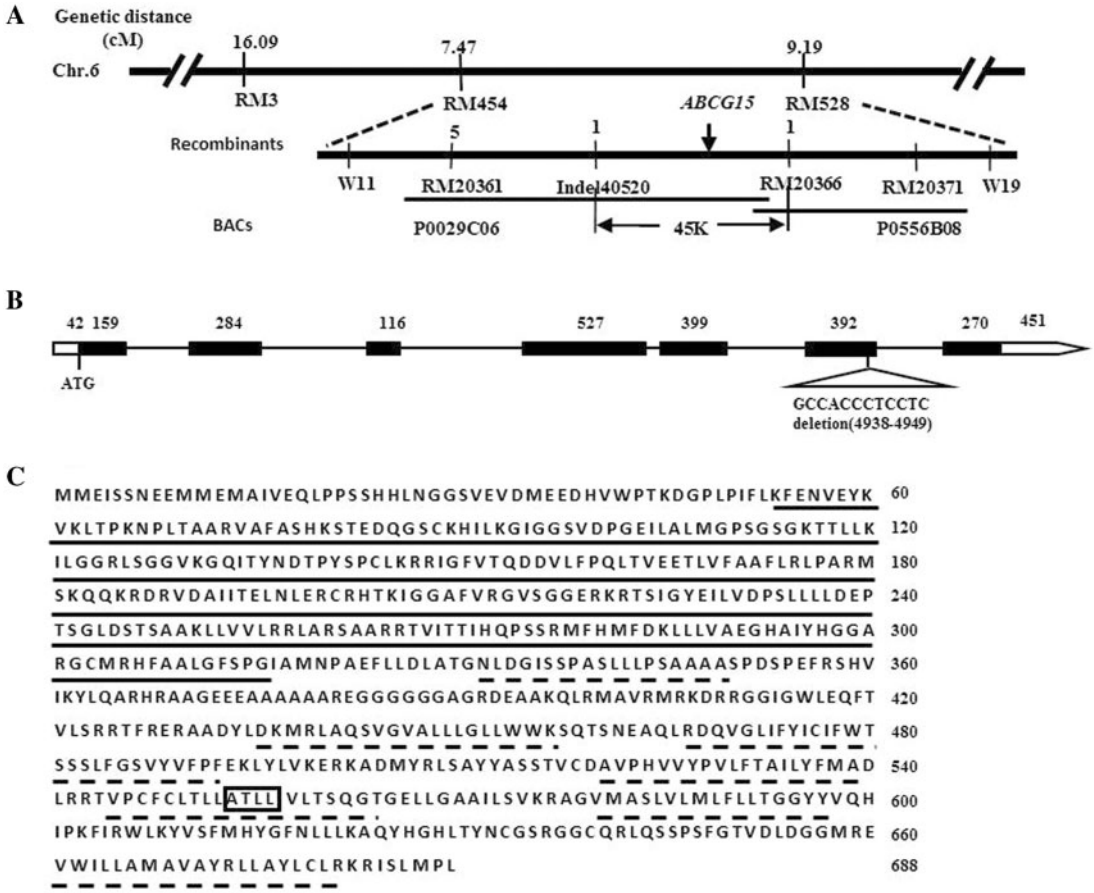

Fig. 5 Mapping-based cloning and analysis of *ABCG15*. (A) Fine mapping of the *ABCG15* gene. cM, centiMorgan. (B) The schematic represents the exon (solid black box), intron (black lines) and untranslated region (UTR; empty box) of *ABCG15*. The number represents the length of the UTR or exon. The 12 nucleotides in the sixth exon represent the 12 nucleotide deletion in *abcg15*. (C) The amino acid sequence of ABCG15 with the predicted ABC transporter domain (solid underline) and the predicted transmembrane domain (dashed underline). The four amino acids (boxed) are the four deleted amino acids in *abcg15*.

respectively. This suggests that ABCG15 is conserved in land plants.

Loss-of-function mutations in Arabidopsis *ABCG26/WBC27*, the putative ortholog of rice *ABCG15*, showed a similar phenotype to the rice *abcg15* mutant with regard to pollen exine formation, suggesting that rice ABCG15 and Arabidopsis ABCG26 might share conserved protein functions. Therefore, we further checked the expression of *ABCG15*-related genes in reproductive tissues of other plants in the available expression databases (www.plexdb.org). The expression of two genes was detected in reproductive tissue, including *Medtr5g103980* in *Medicago truncatula* and *POPTR_0001s37950.1* in *Populus trichocarpa*. *Medtr5g103980* was highly expressed in flower, and *POPTR_0001s37950.1* was only detected in male catkins. This suggests that ABCG15 might have an evolutionarily conserved function. Together, phylogenetic analysis and the expression data suggest that ABCG15 is not only conserved in protein sequence, but also might be conserved in protein function during plant male reproductive development in evolution.

Major components of wax and cutin are reduced in *abcg15*

ABCG15 encodes an ABC transport protein, and the defective anther cuticle and pollen exine in *abcg15* suggest possible defects in transport of wax, cutin and sporopollenin precursors. To identify the possible substrates of ABCG15 homodimer and/or heterodimers, we performed gas chromatography–mass spectrometry (GC-MS) analysis on the wax and cutin monomers of wild-type and *abcg15* anthers. Equivalent surface areas of the anthers of the wild type and mutant were obtained using the approach developed by Li et al. (2010).

From the GC-MS analysis, the total wax per mm^2 of wild-type anthers was 0.4166 μg (**Fig. 7A**; **Table 1**), which primarily consisted of alkanes, alkenes, fatty acids and four unknown rice wax monomers (URWM1, URWM2, URWM3 and URWM4) (**Table 1**). The dominant monomers were pentacosane (C25 alkane), octacosane (C28 alkane), hentriacontane (C31 alkane) and hexacosane (C26 alkene) (**Fig. 7B**; **Supplementary Table S1**). In contrast, 0.2117 μg mm^{-2} total

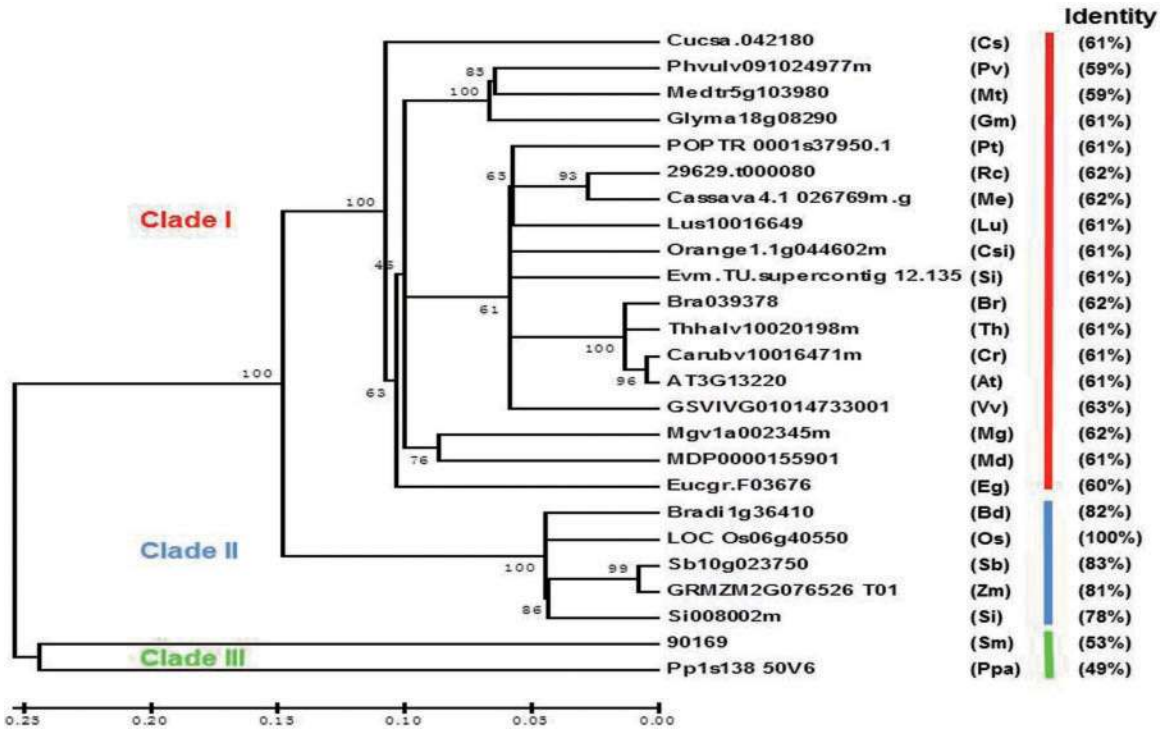

Fig. 6 Protein phylogeny analysis among ABCG15-related members. A Neighbor–Joining phylogeny analysis was performed using MEGA5, based on the alignment result in **Supplementary Fig. S1**. The ABCG15-related sequences are clearly grouped into three clades. Red and blue bars represent clades I and II, respectively, which belong to dicotyledon and monocotyledon flowering plant groups. The green bar represents clade III, which includes *Selaginella moellendorffii* and *Physcomitrella patens*. The numbers at the nodes indicate the bootstrap value. The percentage identities represent the similarity of two sequences between corresponding species and rice. Ac, *Aquilegia coerulea*; At, *Arabidopsis thaliana*; Bd, *Brachypodium distachyon*; Br, *Brassica rapa*; Cs, *Cucumis sativus*; Csi, *Citrus sinenis*; Cr, *Chlamydomonas reinhardtii*; Eg, *Eucalypptus grandis*; Lu, *Linum usitatissimum*; Me, *Manihot esculenta*; Md, *Malus domestica*; Mg, *Mimulus guttatus*; Mt, *Medicago truncatula*; Gm, *Glycine max*; Os, *Oryza sativa*; Pp, *Prunus persica*; Ppa, *Physcomitrella patens*; Pt, *Populus trichocarpa*; Pv, *Phaseolus vulgaris*; Rc, *Ricinus communis*; Si, *Setaria italica*; Sb, *Sorghum bicolor*; Sm, *Selaginella moellendorffii*; Th, *Thellungiella halophila*; Zm, *Zea mays*.

wax was detected in the *abcg15* anthers, only half of the amount of that in wild-type anthers (**Fig. 7A**; **Table 1**). The main reduction was detected in the dominant monomers: octacosane (C28 alkane), hentriacontane (C31 alkane) and hexacosene (C26 alkene), and the monomers with low levels in the wild type also showed significant reduction in *abcg15*, such as linolenic fatty acid (C18:3 FA), docosanoic fatty acid (C22:0 FA), tritriacontane (C33 alkane) and heptacosanol (C27 fatty alcohol) (**Fig. 7B**). Surprisingly, the quantities of URWM1, URWM2 and URWM4 in the mutant were significantly higher than in the wild type (**Fig. 7B**; **Supplementary Table S1**).

The monomer composition of stem cutin can be analyzed with transesterification of the polyester from delipidated tissue (Bonaventure et al. 2004, Franke et al. 2005). Previous studies also indicated that this approach can be applied to analyze the cutin monomer composition of anther epidermal cells (Jung et al. 2006, Zhang et al. 2008). The GC-MS analysis for the depolymerization products after transesterification showed that the total amount of cutin in the wild type was 0.2333 μg mm^{-2} (**Fig. 7A**), which was mainly composed of C16 and C18 oxygenated fatty acid derivatives (**Fig. 7C**; **Supplementary Table S2**). Three other components could not be identified because of the lack of standards, which were named unknown rice cutin monomers (URCM1, URCM2 and URCM3). The total cutin extracted from *abcg15* anther cuticles was 0.0642 μg mm^{-2}, a decrease of 72% from wild-type levels (**Fig. 7A**; **Supplementary Table S1**). Among the reduced monomers, the 18-OH-9-octadecenoic acid (C18:1 ω-OH acid), 9,10-OH-octadecanedioic diacid (C18 9,10-diOH diacid), 18-OH-9,12-octadeca-dienoic acid (C18:2 ω-OH acid) and 9,10,18-trisOH-octadecanoic acid (C18:0: 9,10,18-trisOH acid) were decreased by at least 60% (**Fig. 7C**; **Supplementary Table S2**), and a significant decrease in the amount of low level monomers was observed in *abcg15*, relative to the wild type (**Fig. 7C**). Based on these data, we predict that *abcg15* is involved in the lipid export pathway required for anther cuticle and pollen exine formation, and that the monomers found to be reduced in *abcg15* are potential substrates of ABCG15 homodimers or heterodimers.

ABCG15 is expressed in the tapetum

abcg15 exhibits defective anther and pollen development, affecting the formation of the exine, tapetum and anther cell walls, but has no defects in vegetative growth or other

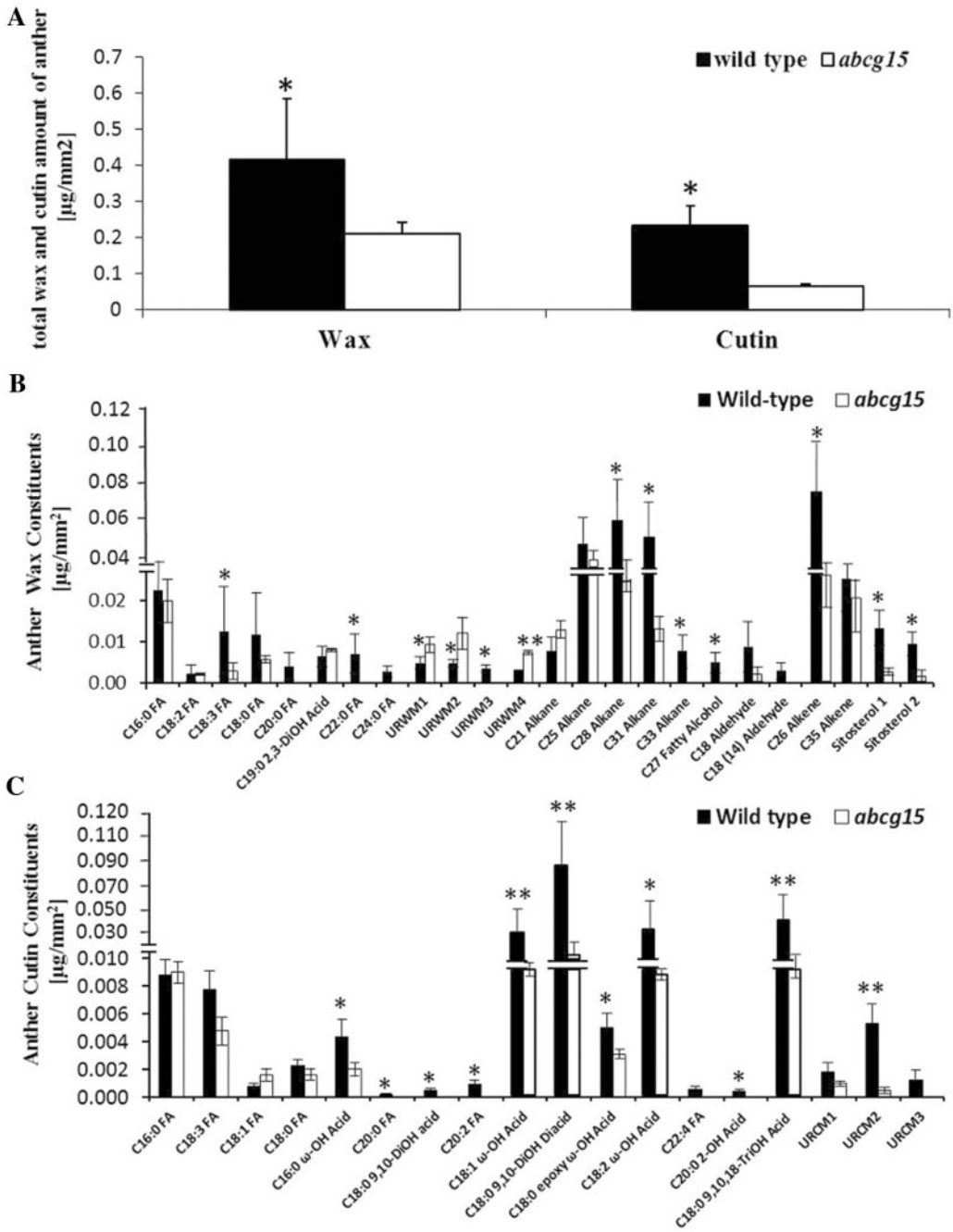

Fig. 7 Wax and cutin constitutions of wild-type and *abcg15* mutant anther cuticle. The total amounts of wax and cutin (A), the amount of wax monomers (B) and cutin monomers (C) per unit anther surface area (μg mm^{-2}) in the wild type (black column) and *abcg15* (white column), respectively. * and ** indicate significant difference at $P < 0.05$ and $P < 0.01$, respectively. Error bars show the SD ($n = 4$). Compound names are abbreviated as follows: C16:0 FA, hexadecanoic fatty acid; C18:2 FA, 9,12-octadecadienoic fatty acid; C18:3 FA, linolenic acid; C18:0 FA, octadecanoic fatty acid; C21 Alkane, heneicosane; C22:0 FA, docosanoic fatty acid; C25 Alkane, pentacosane; C28 Alkane, nonacosane; C31 Alkane, hexatriacontane; C26 Alkene, 9-hexacosene; C33 alkane, Tritriacontane; C35 Alkene,17-pentatriacontene; C27 fatty Alcohol, heptacosanol; C18:1 ω-OH acid, 18-hydroxy-octadecanoic acid; C18:0 9,10-diOH acid, 9,10-dihydroxy-stearic acid; C18:0 epoxy ω-OH acid, 9-epoxy-18-hydroxy-octadecanoic acid. URWM, unknown rice wax monomers; URCM, unknown rice cutin monomers; FA, fatty acid. Acids were analyzed as methyl esters, and hydroxyl groups were analyzed as trimethylsilyl esters.

PCP PLANT & CELL PHYSIOLOGY

Table 1 Wax constitution of anther epidermis between the wild type and *abcg15*

	Wild type [$\mu g\,mm^{-2}$ (%)]	*abcg15* [$\mu g\,mm^{-2}$ (%)]
Acid	0.069 ± 0.051 (16.6)	0.038 ± 0.008 (18.1)
Alkane	0.189 ± 0.065 (45.3)	0.091 ± 0.015 (43.2)
Alkene	0.104 ± 0.029 (25.0)	0.047 ± 0.017 (22.2)
Aldehyde	0.012 ± 0.008 (2.7)	0.002 ± 0.002 (1.0)
Others	0.044 ± 0.013 (10.4)	0.033 ± 0.004 (15.5)
Total	0.417 ± 0.166 (100)	0.212 ± 0.029 (100)

reproductive organ development. Thus, we predicted that *ABCG15* would be expressed exclusively in anthers. To test this, we investigated microarray data on the Rice eFP browser (http://bar.utoronto.ca/efprice/cgi-bin/efpWeb.cgi). *ABCG15* was highly expressed in 10–15 cm inflorescences, but not in other tissues. We further performed reverse transcription–PCR (RT–PCR) and real-time quantitative PCR (RT-qPCR) to investigate *ABCG15* expression patterns. *ABCG15* expression was strongly detected at the young microspore stage, weakly detected at the meiosis stage, and undetectable in root, leaf and the non-reproductive organs including glume, lemma and palea (**Fig. 8A, B**). The high degree of DNA methylation in the *ABCG15* promoter region might play a role in regulating its expression pattern in different organs (http://mpss.udel.edu/rice_sbs/). *TDR* was predicted to regulate *ABCG15* expression positively by binding to the *ABCG15* promoter region (Xu et al. 2010, Choi et al. 2011). *ABCG15* expression was reduced in the young microspore stage and slightly increased in the vacuolated pollen stage in *abcg15* (**Fig. 8B**), which might be caused by the decreased expression of *TDR* in the young microspore stage and increased expression at the vacuolated pollen stage in *abcg15* (**Fig. 9A**). To investigate the spatial and temporal expression patterns of *ABCG15* more precisely, RNA in situ hybridization was performed using wild-type anther sections. *ABCG15* expression was detected specifically in the tapetal cell at the post-meiosis and young microspore stages (**Fig. 8C, D**), with strong expression occurring in the young microspore stage (**Fig. 8D**). In Arabidopsis, the transcription factor AMS regulated *ABCG26/WBC27* expression by binding the E-box in the promoter (Xu et al. 2010, Choi et al. 2011). In rice, *TDR* is the homolog of *AMS*, and seven E-box elements were identified in the upstream 1,000 bp of *ABCG15*. Therefore, *ABCG15* is proposed to be regulated by the tapetum-expressed *TDR*. This supports the finding that *ABCG15* is expressed in the tapetum.

Expression of genes involved in anther and exine development is altered in *abcg15*

As ABCG15 was proposed to function as an ABC transporter downstream of TDR, it was surprising that *TDR* expression was decreased in the *abcg15* mutant (**Fig. 9A**). This raised the question as to whether feedback regulation of gene expression

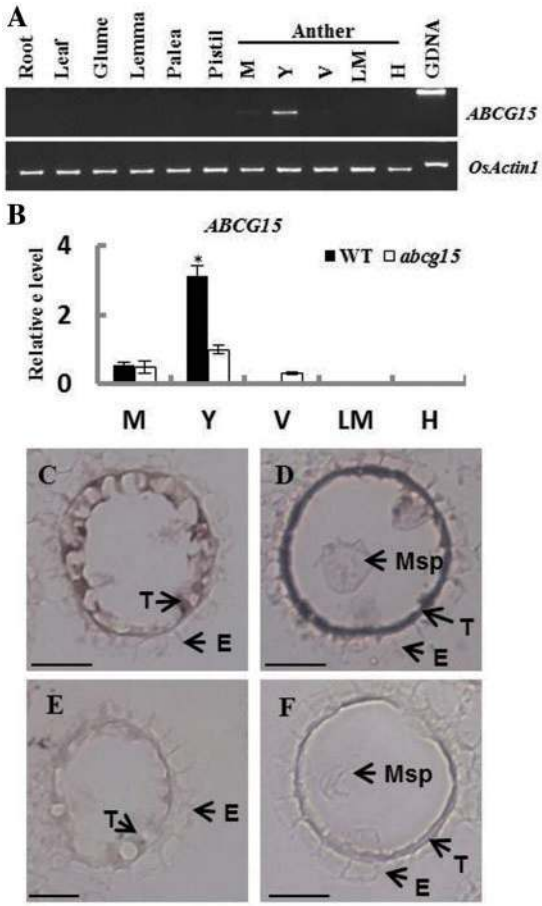

Fig. 8 Expression pattern of *ABCG15*. (A) RT–PCR for spatial and temporal expression analysis of *ABCG15*. (B) RT-qPCR for *ABCG15* expression between the wild type and mutant at meiosis, young microspore, vacuolated pollen, late mitosis and mature pollen stage. (C–F) In situ hybridization using wild-type anther sections. Meiosis stage (C) and (E); young microspore stage (D) and (F). Antisense probe (C) and (D); sense probe (E) and (F). * indicates significant difference at $P < 0.01$. Error bars show the SD ($n = 3$). LM, late mitosis; M, meiosis stage; H, heading flowering stage; MI, middle layer; Ms, microsporocyte; Msp, microspore; E, epidermis; En, endothecium; T, tapetum; V, vacuolated pollen stage; Y, young microspore stage. Bars = 30 μm.

related to lipid metabolism occurs in *abcg15*. Thus, we further investigated expression of additional genes involved in lipid metabolism, including homologs of genes that participate in lipid metabolism in Arabidopsis.

First, we analyzed the expression of major lipid metabolism regulators in wild-type and mutant anthers, including *UDT1*, *GAMYB* and *PTC1*, which are thought to be major regulators in anther and pollen development. Mutations in these genes show phenotypes similar to *abcg15*, with a defective anther cuticle and/or pollen exine (Jung et al. 2005, Li et al. 2006, Aya et al. 2009, Li et al. 2011). Consistent with their previously identified expression patterns in the wild type, the expression of *GAMYB* and *UDT1* was detected in all tested stages (**Fig. 9A, C**).

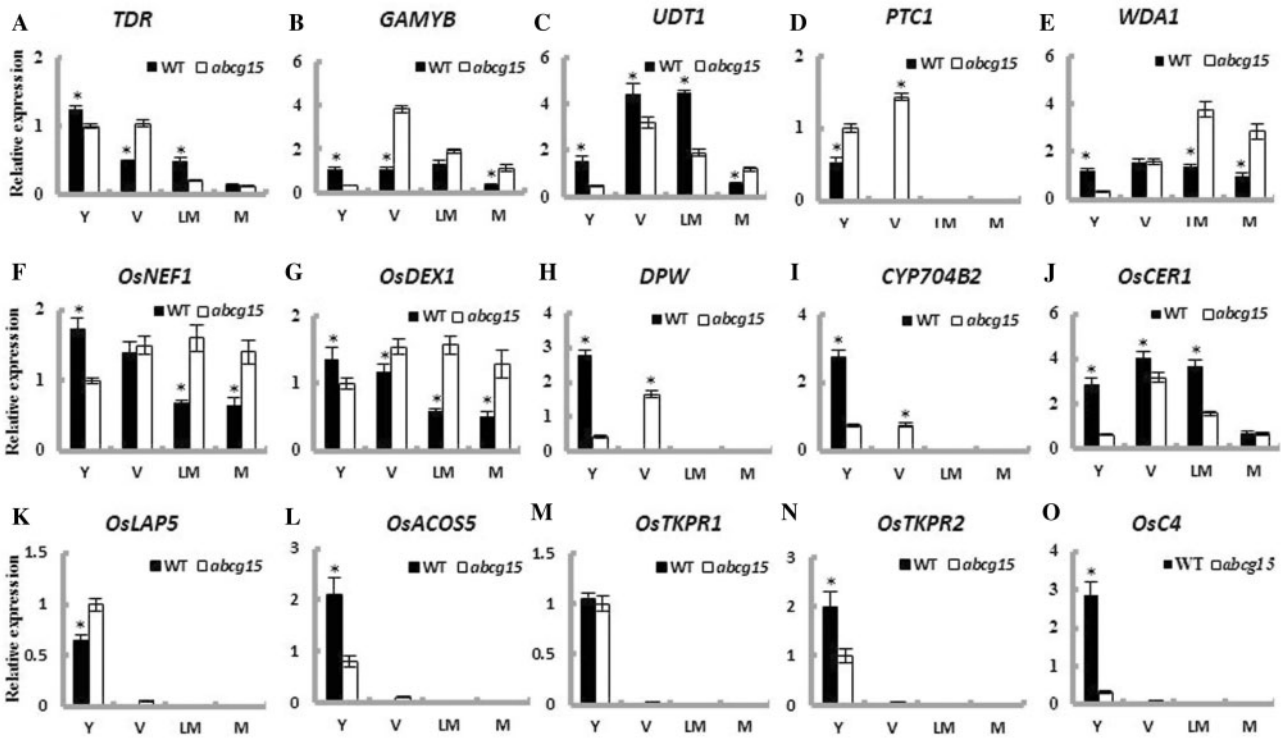

Fig. 9 Gene expression analysis for genes involved in anther lipid metabolism in the wild type and *abcg15*. Expression analysis of *TDR* (A), *GAMYB* (B), *UDT1* (C), *PTC1* (D), *WAD1* (E), *OsNEF1* (F), *OsDEX1* (G), *DPW* (H), *CYP704B2* (I), *OsCER1* (J), *OsC4* (K), *OsACOS5* (L), *OsTKPR1* (M), *OsTKPR2* (N) and *OsLAP5* (O) at the young microspore stage, vacuolated pollen stage, late meiosis stage and mitosis stage in the wild type and *abcg15* by RT-qPCR. *OsActin1* was used a normalizer control. * indicates significant difference at $P < 0.01$. Error bars show the SD ($n = 3$). Y, young microspore stage; V, vacuolated pollen stage; LM, late mitosis stage; M, mature pollen stage.

The expression of *PTC1* was only detected at the young microspore stage (**Fig. 9D**), whereas *TDR* expression in our genetic background (*indica*) was detected from the young microspore to mature pollen stages (**Fig. 9A**). *GAMYB*, *UDT1* and *TDR* expression in *abcg15* was significantly decreased in comparison with the wild type at the young microspore stage (**Fig. 9A–C**), but *PTC1* expression was higher in *abcg15*, which might be caused by negative self-regulation (Li et al. 2011) (**Fig. 9D**). Interestingly, although expression in the wild type was undetectable at the vacuolated pollen stage, *PTC1* expression remained significantly increased in *abcg15* (**Fig. 9D**). At the later stages without *ABCG15* expression (vacuolated pollen, late mitosis and mature pollen stages), the expression of *GAMYB*, *TDR* and *UDT1* was still affected in *abcg15* (**Fig. 9A–C**).

Next, we analyzed the expression of genes involved in lipid biosynthesis in wild-type and *abcg15* anthers, including *WDA1*, *DPW* and *CYP704B2*. Mutants in these genes display defective cuticle and pollen exine development, as observed in the *abcg15* mutant (Jung et al. 2006, Li et al. 2010, Shi et al. 2011). We also analyzed the expression of homologs of Arabidopsis *NEF1*, *DEX1*, *CER1*, *ACOS5*, *TKPR1/2*, *LAT5/PSKB* and *LAT6/PSKA* between the wild type and *abcg15*. Arabidopsis NEF1 and DEX1 are thought to be involved in lipid biosynthesis and to play a role in pollen primexine assembly (Paxson-Sowders et al. 2001, Ariizumi et al. 2004). Arabidopsis CER1 is thought to function in the conversion of long-chain aldehyde to alkane for wax biosynthesis (Aarts et al. 1995, Bourdenx et al. 2011). ACOS5, LAP5/PKSB and LAP6/PKSA, together with TKPR1/2, yield hydroxylated α-pyrone polyketides that are distinct from fatty acids and may be key components of sporopollenin (Grienenberger et al. 2010). Therefore, these homologs might also be involved in lipid and polyketide biosynthesis in rice anther and/or pollen wall formation. The homologs *OsNEF1*, *OsDEX1*, *OsCER1*, *OsACOS5*, *OsTKPR1/2*, *OsLAT5* and *OsLAP6* shared 60, 64, 54, 64, 63, 59, 65 and 64% amino acid sequence identity with *NEF1*, *DEX1*, *CER1*, *ACOS5*, *TRPK1/2*, *LAT5/PSKB* and *LAT6/PSKA*, respectively. In agreement with the previous expression pattern results (Jung et al. 2006, Li et al. 2010, Shi et al. 2011), we detected *WDA1*, *OsNEF1*, *OsDEX1* and *OsCER1* expression in wild-type anthers at all tested stages (**Fig. 9E–G, J**). *DPW*, *CYP704B2*, *OsCER1*, *OsLAP5*, *OsACOS5* and *OsTKPR1/2* expression was observed at the young microspore stage (**Fig. 9H, I, K, L–N**), suggesting that the homologs might function in anther or microspore development. Interestingly, we did not detect *OsLAP6* expression in anthers at any stage, which was consistent with the expression data in the SBS database. At the young microspore stage, the expression level of all tested genes except *OsLAP5* and *OsTKPR1* in *abcg15* was less than in the wild type (**Fig. 9E–J, L, N**), while the expression of *OsLAP5* was increased in *abcg15*, and *OsTKPR1*

expression showed no difference between the wild type and *abcg15* (**Fig. 9K, M**). At the later stages, the expression of *WDA1*, *OsNEF1*, *OsDEX1* and *OsCER1* was also affected (**Fig. 9E–G, J**).

Then, we investigated the expression of two genes with putative roles in lipid transfer, *OsC6* and *OsC4*. *OsC6* encodes a putative lipid transfer protein (LTP), and was proposed to play a role in lipid trafficking during rice anther and pollen exine formation (Zhang et al. 2010). *OsC4*, encoding another LTP, was thought to be related to lipid transfer, and is specifically expressed in tapetal cells (Tsuchiya et al. 1992, Tsuchiya et al. 1994), and down-regulated in *tdr* (Li et al. 2006). Our RT-qPCR result showed that *OsC4* expression was detected in the wild type at the young microspore stage, and was barely detected in other stages. In *abcg15*, *OsC4* expression was significantly decreased at the young microspore stage, and nearly undetectable at later stages (**Fig. 9O**). Unfortunately, we failed to detect *OsC6* expression by RT-qPCR because appropriate primers were not available, but RT–PCR showed decreased expression in *abcg15*, which was similar to *OsC4* expression in *abcg15* at the young microspore stage (**Supplementary Fig. S4**).

Together, the expression of all tested genes was affected in the *abcg15* mutant, except for *OsTKPR1*, suggesting that a mechanism of homeostasis might exist in anther lipid metabolism.

Discussion

ABCG15 is required for anther cuticle, orbicule and exine formation

Male sterility, including cytoplasmic and genic male sterility, plays an important role in rice yield improvement in hybrid rice breeding (Yang et al. 2009). Here, we identified a male sterility line caused by a spontaneous deletion in *ABCG15*, which encodes a putative ABC transporter. The GC-MS and morphological analyses suggest that ABCG15 plays a critical role in the formation of the anther cuticle, orbicules and pollen exine.

The *abcg15* mutant showed thinner anther cuticle, and failed to form nanoridges on the anther epidermal surface. This suggests that ABCG15 is essential for anther cuticle formation, especially for nanoridge formation. Nanoridges normally exist on the surface of floral organs (Panikashvili et al. 2009), such as sepals, petals and anthers, but the function and composition of nanoridges are not clear. Our GC-MS result showed that the absence of nanoridges in the *abcg15* mutant was correlated with the significant reduction in mid-chain hydroxylated fatty acids, which was not reported for the putative ortholog in Arabidopsis (*ABCG26*). Interestingly, the absence of nanoridges in the Arabidopsis *cyp77a6*, *gapt6* and *dcr* mutants is correlated with the absence of 10,16-dihydroxy hexadecanoic acid in petals (Li-Beisson et al. 2009, Panikashvili et al. 2009). This might be because CYP77A6, GPAT6 and DCR are involved in the formation of cutin precursors carrying 10,16-dihydroxy hexadecanoic acid, whereas, ABCG15, as a putative ABC transporter, might be directly or indirectly involved in the transport of such precursors which were significantly decreased in GC-MS analysis. Therefore, the similar absence of nanoridges in the Arabidopsis *cyp77a6*, *gapt6* and *dcr* mutants as well as the rice *abcg15* mutant could be correlated with the absence of these different hydroxylated fatty acid precursors. On the other hand, the observed tapetum-specific expression seems contradictory to the observed anther cuticle defect. OsC6, an LTP in rice anther, is proposed to bind lipid molecules in the tapetum, and then transfer them to the extracellular space. Although *OsC6* expression is detected in the tapetum, the protein is detected in the tapetum, the anther locule, extracellular spaces between the tapetum and epidermis, and the anther cuticle (Zhang et al. 2010). Therefore, the defective anther cuticle as well as pollen exine in the *abcg15* mutant might be explained by a model in which wax, cutin and sporopollenin precursors are exported from the tapetum to the extracellular space by ABCG15 homodimers/heterodimers, and then LTPs such as OsC6 function in the transfer of those precursors to the cuticle and pollen surface to form the epidermal cuticle and pollen wall surfaces.

In many cereals such as rice and wheat, tapetum cells have orbicules and an orbicular wall, which are absent in Arabidopsis. Among many putative functions, orbicules are often proposed to transport tapetum-derived sporopollenin precursors to the developing microspores for pollen exine formation. However, the molecular and biochemical characterization of orbicules has not been studied extensively. Recent biochemical and genetic studies for some genes that are critical for orbicules and pollen exine formation in rice, such as *TDR*, *PTC1*, *WDA1*, *OsC6* and *DPW*, have suggested that orbicule formation is associated with lipid metabolism. The mutant *abcg15*, with a putative defect in lipid transport, could not form orbicules, further supporting that orbicule formation is associated with lipid metabolism, and possibly that orbicules comprise some monomers that were reduced in the GC-MS analysis. Additionally, the abnormal tapetum degradation observed in *abcg15* may be due to defective lipid metabolism, because the improper lipid accumulation in anthers of some mutants is associated with abnormal tapetum morphology (Ariizumi and Toriyama 2011).

Rice has a pollen exine structure distinct from that of Arabidopsis. Exine in rice has free space between the tectum and nexine, which is filled with pollen coat or tryphine in Arabidopsis (Li and Zhang 2010, Ariizumi and Toriyama 2011). Considering the tapetum-specific expression of *ABCG15* and the putative transport role of ABCG15, the absence of pollen exine in the *abcg15* mutant suggests that ABCG15 is required for the transport of sporopollenin precursors from the tapetum to pollen grains, possibly through orbicule trafficking. The similar defect in pollen exine between *abcg15* and the mutant of Arabidopsis *ABCG26/WBC27* suggests that ABCG15 and ABCG26/WBC27 play a conserved role in exine formation regardless of the structural difference between rice and Arabidopsis. Additionally, the expression of all

tested genes except *OsLAP5* and *OsTKPR1* was decreased in *abcg15* (**Fig. 9A–J, L, N, O**), suggesting a feedback regulation mechanism in rice anther that might maintain lipid metabolism homeostasis to avoid excess lipid accumulation in the tapetum. The expression of *OsTKPR1*was not affected in the *abcg15* mutant, implying that the polyketides yielded by TKPR1 might be independent from ABCG15 homo/heterodimer transport, or that the OsTKPR1 enzyme may have different functions in rice. *LAP6/PKSA* and its homolog in moss (*PpASCL*) is expressed in Arabidopsis anthers and the moss sporophyte, respectively (Colpitts et al. 2011). *LAP6/PKSA* was proposed to play an important role in the biosynthesis of polyketides (Dobritsa et al. 2010, Kim et al. 2010), but expression of its rice homolog *OsLAP6/PKSA* was not detected, suggesting that polyketide synthesis in rice anthers might be partially different from that in Arabidopsis. Overall, these findings improve our understanding of the molecular mechanisms of the lipid metabolism machinery in rice anthers.

The potential ABCG interaction partners for ABCG15, and their possible substrates in rice

ABCG15 encodes a half-size ABCG transporter which requires dimerization to be functional (Rees et al. 2009). We investigated the expression patterns of all half-size ABCG transporters in the rice eFP browser and SBS databases to identify interaction candidates for ABCG15. The expression of 13 genes, including ABCG15, was detected in anther or unopened flower around the young microspore stage. RT-qPCR showed that of the 13 gene interaction candidates, *ABCG1*, *ABCG7*, *ABCG9*, *ABCG10*, *ABCG11*, *ABCG12*, *ABCG14*, *ABCG15*, *ABCG22*, *ABCG26* and *ABCG27* were expressed in the wild-type anther at the young microspore stage (**Supplementary Fig. S5**). Of these anther-expressed genes, all showed altered expression levels in *abcg15* compared with wild-type levels, except *ABCG1* and *ABCG7*. In Arabidopsis, *ABCG11/WBC11* and *ABCG12/CER5* (the homologs of rice *ABCG12* and *ABCG26*) function in cuticle formation and are thought to function in lipid transport in the leaf and stem epidermis (Pighin et al. 2004, Bird et al. 2007, Panikashvili et al. 2007, McFarlane et al. 2010). Therefore, rice ABCG12 and ABCG26 are likely to be involved in lipid transport. Therefore, the proteins encoded by the anther-expressed ABCG transporter genes with altered expression in the *abcg15* mutant, particularly rice ABCG12 and ABCG26, are considered the top candidates for interaction with ABCG15. It will be interesting to identify proteins that interact with ABCG15 in vivo in further studies such as bimolecular fluorescence complementation (BiFC) and genetic analyses.

The characterized transporters in the ABCG subfamily have a wide range of substrates, including ABA (Kang et al. 2010, Kuromori et al. 2010), UDP-glucose (M.D. Huang et al. 2009), indole-3-butyric acid (IBA) (Ruzicka et al. 2010) and fatty acids (Pighin et al. 2004). Our study indicates that the wax and cutin monomers whose levels were reduced in *abcg15* by GC-MS analyses are potential substrates of ABCG15 homodimers or heterodimers, and the main components of exine (fatty acids, phenolics and/or polyketides) could be the substrates of ABCG15 homodimers or heterodimers. Due to the similar loss of exine in the rice *abcg15* and Arabidopsis *abcg26* mutants, these proteins may share some functional conservation between monocots and dicots, and these homodimers or heterodimers might have similar substrates which are essential for exine formation. However, because the Arabidopsis *abcg26* mutant did not show anther cuticle defects like the *abcg15* rice mutant (**Supplementary Fig. S6**), ABCG15 may have additional function(s) in the transport of anther metabolites required for normal cuticle formation in rice. This might be because ABCG15 could interact with multiple half-size ABCG transporters for the transport of different substrates required for exine and cuticle formation, while Arabidopsis ABCG26 may have more limited interactions or function solely as a homodimer. Alternatively, because the precursors required for cuticle formation could uniquely be synthesized in rice tapetum cells and absent from Arabidopsis tapetum, this would allow for the export of these cuticle substrates from the rice tapetum by ABCG15 homo/heterodimers and the cuticle defects to be observed specifically in the rice *abcg15* mutant.

Materials and Methods

Mutant material and growth conditions

abcg15 plants and the F_2 mapping populations, generated from a cross between *abcg15* and *9311*(*Indica*) or *Nipponbare* (*Japonica*), were grown in paddies of the Rice Research Institute of Sichuan Agricultural University and Lingshui, Hainan.

Characterization of the mutant phenotype

Thin sections were performed for the anther development analysis as described by Li et al. (2006). For SEM, samples at different stages were pre-fixed in 0.1 M sodium phosphate buffer containing 2.5% glutaraldehyde (pH 6.8) overnight at 4°C, then rinsed twice using 0.1 M phosphate buffer (pH 6.8). Samples were then fixed at least overnight at 4°C in 0.1 M sodium phosphate buffer containing 2% osmium tetroxide. The samples were dehydrated using an acetone series from 30 to 100% and then exchanged three times with isoamyl acetate. The fixed samples were processed for critical point drying using liquid CO_2, and gold coated. The samples were examined with a JEM-1200 EX scanning electron microscope (Hitachi). Arabidopsis SEM anther samples were prepared as described by Quilichini et al. (2010).

For TEM, the anthers of the wild-type and the mutant at different stages were fixed at least overnight in cacodylate buffer (pH7.2), which contained 2% paraformaldehyde and 2% glutaraldehyde. The samples were rinsed with the same buffer and post-fixed for 1–2 h in 2% OsO4 in phosphate-buffered saline (PBS), pH 7.2. Following ethanol dehydration, samples were embedded in acrylic resin (London Resin

Company). Ultrathin sections were collected on uncoated nickel grids, double stained with 4% uranyl acetate, and pictures were taken at 60–80 kV with a Tecnai G2 F20 transmission electron microscope (FEI).

Analysis of anther wax and cutin constituents

Wax and cutin from anthers were analyzed as described previously (Jung et al. 2006). Assuming a cylindrical body for rice anthers, the surface area was determined from pixel numbers in microscopy images (Li et al. 2010), and the number of anthers used for GC-MS analysis was 100 times the number calculated by the whole sample weight divided by the weight of 100 anthers. Approximately 15–25 mg of fresh anther (corresponding to 6–10 mg of freeze-dried anther material) with 80–140 mm^2 anther surface area from the wild-type plants were submerged in 700 µl of chloroform, spiked with 10 µg of tetracosane (Fluka) as the internal standard, for 1 min. The resulting chloroform extract was transferred to a new glass vial. The solvent was evaporated under a gentle stream of nitrogen. Compounds containing free hydroxyl and carboxyl groups were converted to their trimethylsilyl ethers and esters with 0.2 ml of bis-(*N*,*N*-trimethylsilyl)-tri-fluoroacetamide (Sigma-Aldrich) in 0.2 ml of pyridine for 40 min at 70°C in an infrared heating apparatus before GC-FID (Agilent 6890N gas chromatograph) and GC-MS (Agilent gas chromatograph coupled to an Agilent 5973N quadrupole mass selective detector) analyses. Monomers were identified from their electron ionization–mass spectrometry spectra (70 eV, *m*/*z* 50–700) after GC separation [column 30 m × 0.32 mm × 0.1 µm film thickness (DB-1; J & W Scientific)]; on-column injection at 50°C, oven temperature at 50°C for 2 min, increasing at 40°C min^{-1} to 200°C, 2 min at 200°C, increasing at 3°C min^{-1} to 310°C, 30 min at 310°C, and helium carrier gas at 2 ml min^{-1}). Quantification of wax monomers was accomplished with an identical GC system combined with a flame ionization detector.

Analysis of the monomer composition of the anther polyester was performed as described by Franke et al (2005).To ensure complete extraction of all soluble lipids, anthers that had been used in the wax extraction were re-extracted in 1 ml of chloroform/methanol (1 : 1 v/v) for several hours. This extraction step was repeated four times before the anthers were dried at room temperature. The delipidated anthers were then depolymerized using transesterification in 1 ml of 1 N methanolic HCl for 2 h at 80°C. After the addition of 2 ml of saturated $NaCl/H_2O$, the hydrophobic monomers were subsequently extracted three times with 1 ml of hexane spiked with 10 µg of dotriacontane (Fluka) as an internal standard. The organic phases were combined, the solvent evaporated, and the remaining sample derivatized as described above. GC-MS and GC-FID analysis were performed as for the wax analysis using a modified GC temperature program: on-column injection at 50°C, oven temperature of 2 min at 50°C, increasing at 10°C min^{-1} to 150°C, 1 min at 150°C, increasing at 3°C min^{-1} to 310°C.

Complementation of the *abcg15* mutant

For functional complementation, an ~8 kb genomic DNA fragment containing the entire OsABCG15 coding region and ~2 kb of upstream sequence was amplified from the wild type by PCR amplification using primers Q51 and Q52. The DNA fragment was subcloned into the binary vector pCAMBIA1300 to generate the p1300-ABCG15 construct using *Kpn*I and *Eco*RI restriction enzymes. The resulting construct was introduced into *Agrobacterium* EHA105 and transformed into the calli induced from young panicles of *abcg15*.

In situ hybridization

To generate an *ABCG15*-specific antisense probe, a 350 bp (Q46 and Q47) fragment at the 3′-untranslated region of full-length cDNA amplified from wild-type cDNA using ABCG15-specific primers was cloned into PSK vector by *Sal*I and *Hin*dIII restriction enzymes, and then transcribed with T7 RNA polymerase. In situ hybridizations were performed as previously described (Chen et al. 2002). The primers are listed in **Supplementary Table S4**.

RT–PCR and qPCR assay

The total RNA of root, leaf, glume, lemma, palea and anther at different stages was isolated using a Qiagen RNA plant mini kit with on-column DNase digestion (Qiagen). A 2 µg aliquot of total RNA was used for reverse transcription by M-MLVRT (Promega) with oligo(dT18) primer, and 1 µl of reverse transcripase product diluted by 20 µl of ddH_2O was used as template for PCR. For qPCR assay, three technical replicates and three biological replicates were applied for each gene expression analysis. A 600 ng aliquot of total RNA was reverse transcribed by a Primescript RT reagent kit with gDNA eraser (TAKARA). The cDNA diluted to 200 ng $µl^{-1}$ was used for qPCR assay with each gene-specific primer and SsoFast EvaGreen supermix (Bio-Rad) on a Bio-Rad CFX96 real-time system. The reaction was performed at 95°C for 1 min, 40 cycles of 95°C for 10 s, and 58°C for 30 s. All primers for RT–PCR and qPCR are listed in **Supplementary Table S4**.

Phylogenetic analysis

The ABCG15-related amino acid sequences in different species were identified by Phytozome Blast (www.phytozome.net) with default parameters using the full-length amino acid of ABCG15 as a query, and the sequences were aligned with Clustalw2 (Goujon et al. 2010). The phylogenetic tree was generated by the MEGA5 program using the Neighbor–Joining method with default parameters besides 1,000 bootstrap replications (Tamura et al. 2011).

Supplementary data

Supplementary data are available at PCP online.

Funding

This work was supported by the National Natural Science Foundation of China [31025017, 30971763].

Acknowledgments

We thank Sheila McCormick at UC Berkeley and Shuizhang Fei at Iowa State University for editing and comments on the manuscript, and Xuemei Chen at UC Riverside for providing facilities and advice for in situ hybridization.

References

Aarts, M.G., Hodge, R., Kalantidis, K., Florack, D., Wilson, Z.A., Mulligan, B.J. et al. (1997) The *Arabidopsis* MALE STERILITY 2 protein shares similarity with reductases in elongation/condensation complexes. *Plant J.* 12: 615–623.

Aarts, M.G., Keijzer, C.J., Stiekema, W.J. and Pereira, A. (1995) Molecular characterization of the CER1 gene of *Arabidopsis* involved in epicuticular wax biosynthesis and pollen fertility. *Plant Cell* 7: 2115–2127.

Ahlers, F., Bubert, H., Steuernagel, S. and Wiermann, R. (2000) The nature of oxygen in sporopollenin from the pollen of *Typha angustifolia* L. *Z. Natureforsch. C* 55: 129–136.

Ahlers, F., Lambert, J. and Wiermann, R. (2003) Acetylation and silylation of piperidine solubilized sporopollenin from pollen of *Typha angustifolia* L. *Z. Naturforsch. C* 50: 1095–1098.

Ahlers, F., Thoma, I., Lambert, J., Kuckuk, R. and Wiermann, R. (1999) ^{1}HNMR analysis of sporopollenin from Typha angustifolia. *Phytochemistry* 50: 1095–1098.

Ariizumi, T., Hatakeyama, K., Hinata, K., Inatsugi, R., Nishida, I., Sato, S. et al. (2004) Disruption of the novel plant protein NEF1 affects lipid accumulation in the plastids of the tapetum and exine formation of pollen, resulting in male sterility in *Arabidopsis thaliana*. *Plant J.* 39: 170–181.

Ariizumi, T. and Toriyama, K. (2011) Genetic regulation of sporopollenin synthesis and pollen exine development. *Annu. Rev. Plant Biol.* 62: 437–460.

Aya, K., Ueguchi-Tanaka, M., Kondo, M., Hamada, K., Yano, K., Nishimura, M. et al. (2009) Gibberellin modulates anther development in rice via the transcriptional regulation of GAMYB. *Plant Cell* 21: 1453–1472.

Baron, K.N., Schroeder, D.F. and Stasolla, C. (2012) Transcriptional response of abscisic acid (ABA) metabolism and transport to cold and heat stress applied at the reproductive stage of development in Arabidopsis thaliana. *Plant Sci.* 188–189: 48–59.

Bessire, M., Borel, S., Fabre, G., Carraca, L., Efremova, N., Yephremov, A. et al. (2011) A member of the PLEIOTROPIC DRUG RESISTANCE family of ATP binding cassette transporters is required for the formation of a functional cuticle in *Arabidopsis*. *Plant Cell* 23: 1958–1970.

Bird, D., Beisson, F., Brigham, A., Shin, J., Greer, S., Jetter, R. et al. (2007) Characterization of *Arabidopsis* ABCG11/WBC11, an ATP binding cassette (ABC) transporter that is required for cuticular lipid secretion. *Plant J.* 52: 485–498.

Bonaventure, G., Beisson, F., Ohlrogge, J. and Pollard, M. (2004) Analysis of the aliphatic monomer composition of polyesters associated with Arabidopsis epidermis: occurrence of octadeca-cis-6, cis-9-diene-1,18-dioate as the major component. *Plant J.* 40: 920–930.

Bourdenx, B., Bernard, A., Domergue, F., Pascal, S., Leger, A., Roby, D. et al. (2011) Overexpression of *Arabidopsis* ECERIFERUM1 promotes wax very-long-chain alkane biosynthesis and influences plant response to biotic and abiotic stresses. *Plant Physiol.* 156: 29–45.

Chen, G., Komatsuda, T., Ma, J.F., Nawrath, C., Pourkheirandish, M., Tagiri, A. et al. (2011) An ATP-binding cassette subfamily G full transporter is essential for the retention of leaf water in both wild barley and rice. *Proc. Natl Acad. Sci. USA* 108: 12354–12359.

Chen, W., Yu, X.H., Zhang, K., Shi, J., De Oliveira, S., Schreiber, L. et al. (2011) Male sterile2 encodes a plastid-localized fatty acyl carrier protein reductase required for pollen exine development in *Arabidopsis*. *Plant Physiol.* 157: 842–853.

Chen, X., Liu, J., Cheng, Y. and Jia, D. (2002) HEN1 functions pleiotropically in Arabidopsis development and acts in C function in the flower. *Development* 129: 1085–1094.

Choi, H., Jin, J.-Y., Choi, S., Hwang, J.-U., Kim, Y.-Y., Suh, M.C. et al. (2011) An ABCG/WBC-type ABC transporter is essential for transport of sporopollenin precursors for exine formation in developing pollen. *Plant J.* 65: 181–193.

Colpitts, C.C., Kim, S.S., Posehn, S.E., Jepson, C., Kim, S.Y., Wiedemann, G. et al. (2011) PpASCL, a moss ortholog of anther-specific chalcone synthase-like enzymes, is a hydroxyalkylpyrone synthase involved in an evolutionarily conserved sporopollenin biosynthesis pathway. *New Phytol.* 192: 855–868.

de Azevedo Souza, C., Kim, S.S., Koch, S., Kienow, L., Schneider, K., McKim, S.M. et al. (2009) A novel fatty Acyl-CoA synthetase is required for pollen development and sporopollenin biosynthesis in *Arabidopsis*. *Plant Cell* 21: 507–525.

Dobritsa, A.A., Lei, Z., Nishikawa, S., Urbanczyk-Wochniak, E., Huhman, D.V., Preuss, D. et al. (2010) LAP5 and LAP6 encode anther-specific proteins with similarity to chalcone synthase essential for pollen exine development in *Arabidopsis*. *Plant Physiol.* 153: 937–955.

Dobritsa, A.A., Shrestha, J., Morant, M., Pinot, F., Matsuno, M., Swanson, R. et al. (2009) CYP704B1 is a long-chain fatty acid omega-hydroxylase essential for sporopollenin synthesis in pollen of *Arabidopsis*. *Plant Physiol.* 151: 574–589.

Dou, X.-Y., Yang, K.-Z., Zhang, Y., Wang, W., Liu, X.-L., Chen, L.-Q. et al. (2011) WBC27, an adenosine tri-phosphate-binding cassette protein, controls pollen wall formation and patterning in *Arabidopsis*. *J. Integr. Plant Biol.* 53: 74–88.

Feng, J., Lu, Y., Lu, X. and Xu, X. (2001) Pollen development and its stages in rice. *Chinese J. Rice Sci.* 15: 21–28.

Franke, R., Briesen, I., Wojciechowski, T., Faust, A., Yephremov, A., Nawrath, C. et al. (2005) Apoplastic polyesters in Arabidopsis surface tissues—a typical suberin and a particular cutin. *Phytochemistry* 66: 2643–2658.

Gonzalez, C.V., Ibarra, S.E., Piccoli, P.N., Botto, J.F. and Boccalandro, H.E. (2012) Phytochrome B increases drought tolerance by enhancing ABA sensitivity in Arabidopsis thaliana. *Plant Cell Environ.* 35: 1958–1968.

Goujon, M., McWilliam, H., Li, W., Valentin, F., Squizzato, S., Paern, J. et al. (2010) A new bioinformatics analysis tools framework at EMBL-EBI. *Nucleic Acids Res.* 38: W695–W699.

Grienenberger, E., Kim, S.S., Lallemand, B., Geoffroy, P., Heintz, D., de Azevedo Souza, C. et al. (2010) Analysis of TETRAKETIDE alpha-PYRONE REDUCTASE function in *Arabidopsis thaliana* reveals a previously unknown, but conserved, biochemical pathway in sporopollenin monomer biosynthesis. *Plant Cell* 22: 4067–4083.

Hemsley, A.R., Collinson, M.E., Kovach, W.L., Vincent, B.L. and Williams, T. (1994) The role of self-assembly in biological systems: evidence from iridescent colloidal sporopollenin in *Selaginella* megaspore walls. *Philos. Trans. R. Soc. B: Biol. Sci.* 345: 163–173.

Huang, C.F., Yamaji, N., Mitani, N., Yano, M., Nagamura, Y. and Ma, J.F. (2009) A bacterial-type ABC transporter is involved in aluminum tolerance in rice. *Plant Cell* 21: 655–667.

Huang, M.D., Wei, F.J., Wu, C.C., Hsing, Y.I. and Huang, A.H. (2009) Analyses of advanced rice anther transcriptomes reveal global tapetum secretory functions and potential proteins for lipid exine formation. *Plant Physiol.* 149: 694–707.

Jung, K., Han, M.J., Lee, Y.S., Kim, Y.W., Hwang, I., Kim, M.J. et al. (2005) Rice undeveloped tapetum1 is a major regulator of early tapetum development. *Plant Cell* 17: 2705–2722.

Jung, K.H., Han, M.J., Lee, D.Y., Lee, Y.S., Schreiber, L., Franke, R. et al. (2006) Wax-deficient anther1 is involved in cuticle and wax production in rice anther walls and is required for pollen development. *Plant Cell* 18: 3015–3032.

Kang, J., Hwang, J.U., Lee, M., Kim, Y.Y., Assmann, S.M., Martinoia, E. et al. (2010) PDR-type ABC transporter mediates cellular uptake of the phytohormone abscisic acid. *Proc. Natl Acad. Sci. USA* 107: 2355–2360.

Kim, S.S., Grienenberger, E., Lallemand, B., Colpitts, C.C., Kim, S.Y., de Azevedo Souza, C. et al. (2010) LAP6/POLYKETIDE SYNTHASE A and LAP5/POLYKETIDE SYNTHASE B encode hydroxyalkyl alpha-pyrone synthases required for pollen development and sporopollenin biosynthesis in *Arabidopsis thaliana*. *Plant Cell* 22: 4045–4066.

Kuromori, T., Miyaji, T., Yabuuchi, H., Shimizu, H., Sugimoto, E., Kamiya, A. et al. (2010) ABC transporter AtABCG25 is involved in abscisic acid transport and responses. *Proc. Natl Acad. Sci. USA* 107: 2361–2366.

Kuromori, T., Sugimoto, E. and Shinozaki, K. (2011) *Arabidopsis* mutants of AtABCG22, an ABC transporter gene, increase water transpiration and drought susceptibility. *Plant J.* 67: 885–894.

Li, H., Pinot, F., Sauveplane, V., Werck-Reichhart, D., Diehl, P., Schreiber, L. et al. (2010) Cytochrome P450 family member CYP704B2 catalyzes the hydroxylation of fatty acids and is required for anther cutin biosynthesis and pollen exine formation in rice. *Plant Cell* 22: 173–190.

Li, H., Yuan, Z., Vizcay-Barrena, G., Yang, C., Liang, W., Zong, J. et al. (2011) PERSISTENT TAPETAL CELL1 encodes a PHD-finger protein that is required for tapetal cell death and pollen development in rice. *Plant Physiol.* 156: 615–630.

Li, H. and Zhang, D. (2010) Biosynthesis of anther cuticle and pollen exine in rice. *Plant Signal. Behav.* 5: 1121–1123.

Li, N., Zhang, D.S., Liu, H.S., Yin, C.S., Li, X.X., Liang, W.Q. et al. (2006) The rice tapetum degeneration retardation gene is required for tapetum degradation and anther development. *Plant Cell* 18: 2999–3014.

Li-Beisson, Y., Pollard, M., Sauveplane, V., Pinot, F., Ohlrogge. J. and Beisson, F. (2009) Nanoridges that characterize the surface morphology of flowers require the synthesis of cutin polyester. *Proc. Natl Acad. Sci. USA* 106: 22008–22013.

Liu, Z., Bao, W., Liang, W., Yin, J. and Zhang, D. (2010) Identification of gamyb-4 and analysis of the regulatory role of GAMYB in rice anther development. *J. Integr. Plant Biol.* 52: 670–678.

Markus, R. (2006) Introduction. *In* Biology of the Plant Cuticle. pp. 1–8. Blackwell, Oxford.

McCormick, S. (1993) Male gametophyte development. *Plant Cell* 5: 1265–1275.

McFarlane, H.E., Shin, J.J.H., Bird, D.A. and Samuels, A.L. (2010) *Arabidopsis* ABCG transporters, which are required for export of diverse cuticular lipids, dimerize in different combinations. *Plant Cell* 22: 3066–3075.

Panikashvili, D., Savaldi-Goldstein, S., Mandel, T., Yifhar, T., Franke, R.B., Hofer, R. et al. (2007) The *Arabidopsis* DESPERADO/AtWBC11 transporter is required for cutin and wax secretion. *Plant Physiol.* 145: 1345–1360.

Panikashvili, D., Shi, J.X., Bocobza, S., Franke, R.B., Schreiber, L. and Aharoni, A. (2010) The Arabidopsis DSO/ABCG11 transporter affects cutin metabolism in reproductive organs and suberin in roots. *Mol. Plant* 3: 563–575.

Panikashvili, D., Shi, J.X., Schreiber, L. and Aharoni, A. (2009) The Arabidopsis DCR encoding a soluble BAHD acyltransferase is required for cutin polyester formation and seed hydration properties. *Plant Physiol.* 151: 1773–1789.

Panikashvili, D., Shi, J.X., Schreiber, L. and Aharoni, A. (2011) The *Arabidopsis* ABCG13 transporter is required for flower cuticle secretion and patterning of the petal epidermis. *New Phytol.* 190: 113–124.

Paxson-Sowders, D.M., Dodrill, C.H., Owen, H.A. and Makaroff, C.A. (2001) DEX1, a novel plant protein, is required for exine pattern formation during pollen development in Arabidopsis. *Plant Physiol.* 127: 1739–1749.

Pighin, J.A., Zheng, H., Balakshin, L.J., Goodman, I.P., Western, T.L., Jetter, R. et al. (2004) Plant cuticular lipid export requires an ABC transporter. *Science* 306: 702–704.

Quilichini, T.D., Friedmann, M.C., Samuels, A.L. and Douglas, C.J. (2010) ATP-binding cassette transporter G26 is required for male fertility and pollen exine formation in *Arabidopsis*. *Plant Physiol.* 154: 678–690.

Rea, P.A. (2007) Plant ATP-binding cassette transporters. *Annu. Rev. Plant Biol.* 58: 347–375.

Rees, D.C., Johnson, E. and Lewinson, O. (2009) ABC transporters: the power to change. *Nat. Rev. Mol. Cell Biol.* 10: 218–227.

Ruzicka, K., Strader, L.C., Bailly, A., Yang, H., Blakeslee, J., Langowski, L. et al. (2010) *Arabidopsis* PIS1 encodes the ABCG37 transporter of auxinic compounds including the auxin precursor indole-3-butyric acid. *Proc. Natl Acad. Sci. USA* 107: 10749–10753.

Samuels, L., Kunst, L. and Jetter, R. (2008) Sealing plant surfaces: cuticular wax formation by epidermal cells. *Annu. Rev. Plant Biol.* 59: 683–707.

Scott, R.J., Spielman, M. and Dickinson, H.G. (2004) Stamen structure and function. *Plant Cell* 16: S46–S60.

Shi, J., Tan, H., Yu, X.H., Liu, Y., Liang, W., Ranathunge, K. et al. (2011) Defective pollen wall is required for anther and microspore development in rice and encodes a fatty acyl carrier protein reductase. *Plant Cell* 23: 2225–2246.

Tamura, K., Peterson, D., Peterson, N., Stecher, G., Nei, M. and Kumar, S. (2011) MEGA5: molecular evolutionary genetics analysis using maximum likelihood, evolutionary distance, and maximum parsimony methods. *Mol. Biol. Evol.* 28: 2731–2739.

Tsuchiya, T., Toriyama, K., Ejiri, S. and Hinata, K. (1994) Molecular characterization of rice genes specifically expressed in the anther tapetum. *Plant Mol. Biol.* 26: 1737–1746.

Tsuchiya, T., Toriyama, K., Nasrallah, M.E. and Ejiri, S. (1992) Isolation of genes abundantly expressed in rice anthers at the microspore stage. *Plant Mol. Biol.* 20: 1189–1193.

Verrier, P.J., Bird, D., Burla, B., Dassa, E., Forestier, C., Geisler, M. et al. (2008) Plant ABC proteins—a unified nomenclature and updated inventory. *Trends Plant Sci.* 13: 151–159.

Xu, J., Yang, C., Yuan, Z., Zhang, D., Gondwe, M.Y., Ding, Z. et al. (2010) The ABORTED MICROSPORES regulatory network is required for postmeiotic male reproductive development in *Arabidopsis thaliana*. *Plant Cell* 22: 91–107.

Yang, S., Cheng, B., Shen, W. and Xia, J. (2009) Progress of application and bredding on two-line hybrid rice in China. *Hybrid Rice* 72: 5–9.

Zhang, D., Liang, W., Yin, C., Zong, J. and Gu, F. (2010) OsC6, encoding a lipid transfer protein, is required for postmeiotic anther development in rice. *Plant Physiol.* 154: 149–162.

Zhang, D.S., Liang, W.Q., Yuan, Z., Li, N., Shi, J., Wang, J. et al. (2008) Tapetum degeneration retardation is critical for aliphatic metabolism and gene regulation during rice pollen development. *Mol. Plant* 1: 599–610.